TITLE PAGE

Mast cell degranulation increases mouse Mast Cell Protease 4-dependent vasopressor responses to big endothelin-1 but not Angiotensin I.

Laurence Vincent[1], Catherine Lapointe[1], Modou Lo[1], Hugo Gagnon[2], Gunnar Pejler[3], Shinji Takai[4], Robert Day[5] and Pedro D'Orléans-Juste[1*].

[1] Department of Pharmacology and Physiology, Faculté de Médecine et des Sciences de la Santé, Université de Sherbrooke, Sherbrooke, QC, Canada ;
[2] PhenoSwitch Bioscience Inc., Sherbrooke, QC, Canada ; [3] Department of Medical Biochemistry and Microbiology, Uppsala University, Uppsala, Sweden ;
[4] Department of Innovative Medicine, Osaka Medical College, Osaka, Japan ;
[5] Department of Surgery, Division of Urology, Université de Sherbrooke, Sherbrooke, QC, Canada.

* Corresponding author at: Department of Pharmacology and Physiology, Université de Sherbrooke, 3001, 12e Avenue Nord, Sherbrooke, Quebec, Canada, J1H 5N4. E-mail address: labpdj@usherbrooke.ca

RUNNING TITLE PAGE

Running title: Mast cell degranulation enhances big ET-1 pressor response.

Corresponding author:

Pedro D'Orléans-Juste

Department of Pharmacology and Physiology, Université de Sherbrooke,

3001, 12e Avenue Nord, Sherbrooke, Quebec, Canada, J1H 5N4.

E-mail address: labpdj@usherbrooke.ca

Text pages: 35

Tables: 1 (supplement)

Figures: 6 + 1 supplementary figure

References: 44

Words in Abstract: 238

Words in Introduction: 570

Words in Discussion: 1146

Recommended section assignment: Cardiovascular

LIST OF NON-STANDARD ABBREVIATIONS

Angiotensin-converting enzyme (ACE), 7-amino-4-methylcoumarin (AMC), Angiotensin I (Ang I), Angiotensin II (Ang II), big endothelin-1 (big ET-1), bovine serum albumin (BSA), Compound 48/80 (C48/80), endothelin-1 (ET-1), endothelin-1 (1-31) (ET-1 (1-31)), endothelin-converting enzyme (ECE), heart rate (HR), intramuscular (IM), intraperitoneal (IP), intravenous (IV), knock out (KO), mean arterial pressure (MAP), mouse mast cell protease 4 (mMCP-4), neprilysin (NEP), nitric oxide (NO), phosphate buffer solution (PBS), recombinant mMCP-4 (rmMCP-4), variations (Δ), wild-type (WT).

2

ABSTRACT

Mouse mast cell protease 4 (mMCP-4), the murine functional analogue to the human chymase, is a serine protease synthesized and stored in mast cell secretory granules. Our previous studies reported physiological and pathological roles for mMCP-4 in the maturation and synthesis of the vasoactive peptide endothelin-1 (ET-1) from its precursor, big endothelin-1 (big ET-1). The aim of this study was to investigate the impact of mast cell degranulation or stabilization on mMCP-4-dependent pressor responses following the administration of big ET-1 or Angiotensin I (Ang I). In anesthetized mice, mast cell degranulation induced by Compound 48/80 (C48/80) or stabilization by cromolyn enhanced or repressed, respectively, the dose-dependent vasopressor responses to big ET-1 in wild-type (WT) mice but not in mMCP-4 knockout mice in a chymase inhibitor (TY-51469)-sensitive fashion. In addition, mMCP-4-dependent hydrolysis of the fluorogenic substrate Suc-Leu-Leu-Val-Tyr-7-amino-4-methylcoumarin was depleted or enhanced in peritoneal mast cells isolated from mice pre-treated with C48/80 or cromolyn, respectively. Furthermore, C48/80 or cromolyn markedly increased or abolished, respectively, ET-1 (1-31) conversion from exogenous big ET-1 in WT mice peritoneal fluid-isolated mast cells, *in vitro.* Finally, the vasopressor responses to Ang I were unaffected by mast cell activation or stabilization, whereas those induced by the Angiotensin-converting enzyme-resistant Ang I analogue, [Pro[11], D-Ala[12]] Ang I, were potentiated by C48/80. Altogether, the present study shows that mast cell activation enhances the

mMCP-4-dependent vasoactive properties of big ET-1 but not Ang I in the mouse model.

SIGNIFICANCE STATEMENT

The current work demonstrates a significant role for mast cell stability in the cardiovascular pharmacology of big ET-1 but not Ang I in the murine systemic circulation.

INTRODUCTION

Upon activation, mast cells undergo a biphasic secretory response involving the rapid release of pre-stored vasoactive mediators followed by subsequent release of *de novo*-synthesized products, significantly modulating several physiological and pathological pathways (Blank, 2011). Secretion of the serine protease chymase, a major component of the mast cell secretory granules, is notably involved in the maturation of vasoactive factors such as Angiotensin II (Ang II) and endothelin-1 (ET-1) (Fleming, 2006; Nakano *et al.*, 1997), both acting in the regulation of the vascular flow and hemodynamic balance (Rossi, 1999).

Comparative studies in human, hamster, rat, rabbit, dog, pig, and marmoset tissues reported remarkable variations in the Ang II-forming pathways among several organs *in vitro*, suggesting that the chymase contribution to local Ang II generation could be species-dependent (Balcells *et al.*, 1997; Akasu *et al.*, 1998; Kunori *et al.*, 2005). By adopting an *in vitro* mouse model*,* it was shown that, under physiological conditions, Angiotensin-converting enzyme (ACE) is the major Ang II-forming dipeptidyl-carboxypeptidase (Company *et al.*, 2011). Ang II can however, under inflammatory conditions, also be generated *via* mast cell activation by release of the extravascular mouse mast cell protease 4 (mMCP-4) (Company *et al.*, 2011), the closest mouse analogue to human chymase (Pejler *et al.*, 2010). Notably though, whether mast cell activation and secretion of mMCP-4 can modulate the response of the cardiovascular system to Angiotensin I (Ang I) *in vivo* remains to be determined.

The endothelin-converting enzyme (ECE) is located on endothelial cells membrane, but also on a wide variety of cell types such as vascular smooth muscle cells, macrophages and neurons (Davenport *et al.*, 2016). Such cells produce ET-1 through ECE-mediated conversion of big endothelin-1 (big ET-1) (McMahon *et al.*, 1991; Xu *et al.*, 1994). An alternate pathway of ET-1 generation involves mast cell chymase, through the production of an inactive intermediate, endothelin-1 (1-31) (ET-1 (1-31)), as shown in human tracheal smooth muscle cells (Nakano *et al.*, 1997). ET-1 (1-31) is subsequently cleaved by the neprilysin (NEP) to form the vasoactive peptide ET-1 (1-21), which is a prerequisite to exert its pressor properties *in vivo* (Fecteau *et al.*, 2005). We have previously shown a 40% reduction in the pressor responses induced by the administration of big ET-1 in mice genetically deficient for mMCP-4 (mMCP-4 KO) (Tchougounova *et al.*, 2003), demonstrating a dynamic role for chymase in the generation of ET-1 *in vivo* (Houde *et al.*, 2013). Although mMCP-4 metabolizes big ET-1 *in vivo* and Ang I *in vitro* (Fecteau *et al.*, 2005; Fleming, 2006), the impact of acute mast cell activation or stabilization on the hydrolytic properties of mMCP-4 *in vivo* remains uninvestigated. We suggest that mast cell degranulation enhances mMCP-4-dependent cardiovascular responses to big ET-1 in the mouse model *in vivo*.

This study therefore investigated the influence of mast cell degranulation on the chymase-dependent pressor responses to big ET-1 or Ang I in wild-type (WT) or mMCP-4 KO mice. These agonists were tested in mice treated with the mast cell degranulating agent Compound 48/80 (C48/80) (Irman-Florjanc and Erjavec, 1983) or the mast cell stabilizer cromolyn (Samoszuk and Corwin, 2003)

and when applicable with the chymase inhibitor TY-51469 (Koide *et al.*, 2003). Finally, the contribution of degranulated mMCP-4 on the pressor responses to [Pro^{11}, D-Ala^{12}] Ang I, an ACE-resistant analogue (McDonald *et al.*, 2001) was also investigated *in vivo*.

Our study shows that modulation of mast cell activation significantly impacts the hemodynamic responses to big ET-1 but not Ang I.

METHODS

Animals

C57Bl/6 mice genitors were purchased from Charles River Canada (Montreal, QC, Canada) and housed in our facilities. Genitor mMCP-4 KO mice were provided by Dr Gunnar Pejler (Uppsala University, Sweden) and bred in our facility. All animals (male mice, 8-12 weeks old) were kept at constant room temperature (23°C) and humidity (78%) under a controlled 12-hour light/dark cycle, with standard chow and tap water *ad libitum*. Animal care and experimentations were approved by the Ethics Committee on Animal Research of the University of Sherbrooke following the Canadian Council on Animal Care guidelines and the Guide for the Care and Use of Laboratory Animals of the U.S. National Institutes of Health.

Mice were anesthetized by the intramuscular (IM) administration of ketamine/xylazine (87/13 mg/kg). The intraperitoneal (IP) administration of vehicle, C48/80 (1 mg/kg) or cromolyn (50 mg/kg), 5 or 30 min respectively prior to further experimentations, was performed (Röhlich *et al.*, 1971; Skedinger *et al.*, 1987; Tariq *et al.*, 2006).

Hemodynamic monitoring in anesthetized mice

The method was performed as previously described (Houde *et al.*, 2013). Anesthetized mice were cannulated with a polyethylene catheter *via* the left jugular vein for intravenous (IV) administration, and the right carotid artery for hemodynamic recordings using the Blood Pressure Analyzer 200A (Digi-Med,

Louisville, KY). Following the surgery, the mice were allowed a 15 min stabilization period before the IV injection of either big ET-1 (Phoenix Pharmaceuticals Inc., Burlingame, CA), ET-1 (1-31) (Peptide Institute, Osaka, Japan), ET-1 (Enzo Life Sciences Inc. Farmingdale, NY), Ang I (TOCRIS Bioscience, Ellisville, MO) or [Pro^{11}, D-Ala^{12}] Ang I (American Peptide Company; Sunnyvale, CA) with doses ranging from 0.001 nmol/kg to 10 nmol/kg (D'Orléans-Juste *et al.*, 2008). Each mouse was administered a unique dose and blood pressure parameters were continuously monitored for a maximum of 20 min before the mice were sacrificed by cervical dislocation. All data were analyzed using the DMSI-400 System Integrator software (Digi-Med® System Integrator™, Louisville, KY). Blood pressure variations (Δ) obtained after the injection of each vasopressor were calculated as the difference between blood pressure increases post-injection and basal pressure recorded prior to administration of each agent. Recording of heart rate (HR) was initiated at the time of agonist administration. In another series of experiments, the specific chymase inhibitor TY-51469 (10 mg/kg) (Toa Eiyo limited, Osaka, Japan) was administered intravenously 20 min before drug administration.

Peritoneal mast cells isolation

Mast cells from the peritoneal cavity were isolated from vehicle, C48/80 or cromolyn pre-treated mice (as described above) and used for measurement of chymase activity as previously reported (Semaan et al., 2015). Mice anesthetized with ketamine/xylazine (87/13 mg/kg IM) were injected with 5 ml of isolation buffer (PBS pH 7.4 containing 1 mg/ml of BSA and 0.5 mg/ml of heparin) in the

peritoneal cavity. The peritoneal fluids were collected following a 1 min abdominal massage and centrifuged at 200 g for 5 min. Pellets were suspended in 1 ml of RPMI-1640 medium containing 2 mM of L-glutamine, 100 U/ml of penicillin and 1 mg/ml of BSA and subsequently incubated for 1h at 37°C in tissue culture dishes 35 X 10 mm in order to sediment and allow adherence to the plastic surface of the dish the macrophages and leukocytes thus allowing a purification of the mast cells. RPMI-1640 medium and non-adherent cells were collected and centrifuged at 200 g for 5 min. Pellets were suspended in 1 ml of isolation buffer and cells were counted using a hemocytometer (zoom in to 40x magnification) according to the Moore & James method with toluidine blue (0.038%) (Moore and James, 1953). A final centrifugation was performed at 200 g for 5 min and pellets were suspended in PBS (pH 8) at a concentration of 1 x 10^4 cells/µl.

Activation of the recombinant enzymes

Recombinant mMCP-4 was expressed in *S2 drosophila* cells and purified as previously described (Semaan *et al.*, 2015). The recombinant enzymes were thawed and diluted to a concentration of 20 µg/ml in maturation buffer (50 mM MES, 1 mg/ml BSA, pH 5.5). Active murine cathepsin C (R&D Systems, Minneapolis, MN) was diluted to 20 µg/ml in cathepsin C buffer (50 mM MED, 50 mM NaCl, 5 mM DTT, pH 5.5). Activation was performed by adding equal volumes of recombinant chymase and cathepsin C, adding 50 µg/ml heparin and incubating 1h at room temperature. mMCP-4 activation was stopped with NEM (3 mM) and diluted with assay buffer (20 mM Tris, 200 µM KCl, 0.02% Triton X-100,

pH 9.0) to bring the recombinant enzyme concentration to 2 µg/ml or 5 µg/ml, and 5 min was allowed to completely stop the cathepsin C-dependent reaction.

Measurement of chymase enzymatic activity

Activated rmMCP-4 at concentrations of 30.85 nM (100 ng/well) and 154.32 nM (500 ng/well), in absence or presence of C48/80 (12 µM), cromolyn (600 µM) or TY-51469 (10 µM), or mast cells (1 x 10^5 cells), were incubated in 96 well plates with the fluorogenic substrate, Suc-Leu-Leu-Val-Tyr-7-amino-4-methylcoumarin (AMC) (10 µM) (Peptide Institute inc., Osaka, Japan), The fluorescence of the released AMC molecule, as chymotrypsin-like activity, was then measured in duplicate with an Infinite M1000 spectrophotometer (Tecan Group Ltd., Männerdorf, Swiss) with λ_{ex} = 370 nm and λ_{em} = 460 nm, at 37°C for up to 20 min.

Mast cell-specific conversion of big ET-1 to ET-1 (1–31) in vitro

Big ET-1 (15 µM) was incubated with 1 x 10^5 mast cells. Thiorphan (1 µM), a NEP inhibitor, was added to the reaction in order to block conversion of ET-1 (1-31) to ET-1. C48/80 (1 µM) or cromolyn (20 µM) was added to the medium and incubated for 20 min at 37°C. Formic acid (4%) was added to lower the pH and to completely stop the enzymatic reaction.

Peptide samples (200 µl per tube) were analyzed via LC-MS/MS analysis by PhenoSwitch Bioscience. Each sample was loaded on Strata-X polymeric reversed-phase columns. Peptides were eluted twice with 350 µl 75% acetonitrile, 2% formic acid. Eluates were dried, samples were then suspended in

50 µl of H_2O with 2% formic acid and 5 µl was injected on a Halo peptide C18 50 x 0.5 mm column eluted with water, 3% DMSO, 0.2% formic acid (mobile phase A) and acetonitrile, 3% DMSO, 0.2% formic acid (mobile phase B). The flow rate was 25 µl/min for the 2.5 min duration and gradients started at 10% mobile phase B. ET-1, ET-1 (1-31) and big ET-1 were monitored by product ion acquisition on TTOF5600 from AbSciex.

Statistical analysis

All quantitative results are presented as the mean ± S.E.M. All graphical and statistical analysis were conducted on GraphPad Prism 8 software (GraphPad Software, La Jolla, CA). Statistical significance was determined with Student's *t* test for comparisons of two samples, or one-way analysis of variance (ANOVA) with Dunnett's multiple comparison tests for three or more sample sets. Statistical significance was reached when the "P" value was below 0.05 and one symbol (*) represents $p<0.05$, two (**) show that $p<0.01$, and three (***) show that $p<0.001$.

RESULTS

*No differences in basal hemodynamic parameters in WT and mMCP-4 KO mice
following the intraperitoneal administration of C48/80 or cromolyn.*

Prior to drug injections, the basal hemodynamic parameters were
measured in anesthetized mice treated with either vehicle, C48/80 or cromolyn.
Mean, systolic and diastolic arterial pressure, HR and arterial pulse pressure
were similar in both groups regardless of the pharmacological agent
administered (Supplement Table 1).

*Interfering with mast cell stability modulates the mMCP-4-dependent
hemodynamic responses to big ET-1.*

The dose-dependent increases in mean arterial pressure (MAP) after
bolus administrations (IV) of big ET-1 were compared in WT and mMCP-4 KO
mice, treated intraperitoneally with C48/80 (1 mg/kg) or cromolyn (50 mg/kg).
C48/80 potentiated the maximal increases of the MAP induced by exogenous
big ET-1 at doses ranging from 0.01 to 1 nmol/kg ($p<0.05$), with no variations of
HR at all doses tested. In contrast, at the same doses, pressor responses to big
ET-1 were markedly reduced in cromolyn-treated WT ($p<0.05$) but not in mMCP-
4 KO mice (Fig. 1A and B). Figure 1C and D show that the potentiating or
repressing effects of C48/80 or cromolyn, respectively, occur throughout the
sustained pressor responses to big ET-1 in WT mice. Finally, no effects of
C48/80, cromolyn or mMCP-4-deficiency on HR in response to big ET-1 were
observed (Fig. 1E and F).

Interfering with mast cell stability does not influence the hemodynamic responses to big ET-1 metabolites ET-1 (1-31) or ET-1.

A specific chymase inhibitor, TY-51469 (10 mg/kg, IV), suppressed the mMCP-4 contribution to the pressor responses to big ET-1 in WT mice ($p<0.001$), regardless of induction of mast cell degranulation or stabilization (Fig. 2A). ET-1 (1-31) (1 nmol/kg) and ET-1 (0.5 nmol/kg) induced similar hemodynamics in WT mice treated with vehicle, C48/80 or cromolyn (Fig. 2B). Thus, mast cell stability plays no significant role in the vasoactive effects of the latter two metabolites.

C48/80 and cromolyn increase or abolish, respectively, mast cells derived mMCP-4-dependent conversion of big ET-1 to ET-1 (1-31).

In a first series of specificity experiments, concentration-dependent chymase activity of recombinant mMCP-4 was assessed (Supplement Figure 1). Furthermore, the latter serine protease activity was not modified by C48/80 or cromolyn yet abolished by TY-51469 (Fig. 3A).

The hydrolysis of the fluorogenic substrate was subsequently measured in peritoneal fluid-isolated mast cells from WT and mMCP-4 KO mice pre-treated with either vehicle, C48/80 or cromolyn. Figure 3B shows that C48/80 markedly reduced ($p<0.001$) the mast cell's chymase-like activity, suggesting a lower content in mMCP-4 following the induction of degranulation. On the other hand, cromolyn produced an increase in hydrolytic activity ($p<0.05$), suggesting a greater enzyme content in stabilized mast cells. We had previously reported that

WT mouse peritoneal mast cells possess mMCP-4-dependent hydrolytic activity (Semaan *et al.*, 2015; Desbiens *et al.*, 2019). Worthy of notice, 1 x 10^5 isolated peritoneal mast cells were equivalent to a concentration of 150 nM of the recombinant mMCP-4 in terms of chymase specific-hydrolysis.

Finally, C48/80 and cromolyn, respectively enhanced or abolished the production of ET-1 (1-31) from exogenous big ET-1 in mast cells isolated from WT mice peritoneal fluid (*p*<0.001 and *p*<0.05, respectively) (Fig. 3C). ET-1 (1-31) generation did not occur in peritoneal mast cells derived from mMCP-4 KO mice (*p*<0.001) (Fig. 3C).

C48/80 or cromolyn do not affect hemodynamic responses to Ang I in anesthetized mice.

The absence of mMCP-4-specific contributions in the generation of the potent vasopressor peptide Ang II is shown in Figure 4. Ang I (0.001 to 0.5 nmol/kg) administered to either WT or mMCP-4 KO mice elicited similar vasopressor responses (Fig. 4A). Higher doses of Ang I triggered tachycardia in the anesthetized mouse model (data not shown). Figure 4B and C show no effects of C48/80 or cromolyn on duration of the pressor responses to Ang I (0.01 nmol/kg), either in WT or mMCP-4 KO mice. Further, no effects of C48/80, cromolyn or mMCP-4-deficiency on HR in response to Ang I were monitored (Fig. 4D and E).

Mast cell degranulation modulates the mMCP-4-dependent hemodynamic responses to [Pro^{11}, D-Ala^{12}] Ang I.

In contrast to Ang I, administration of the ACE-resistant analogue [Pro^{11}, D-Ala^{12}] Ang I induced pressor responses with greater amplitude and duration in WT mice when compared to their mMCP-4 KO congeners ($p<0.01$), unmasking a chymase-dependent contribution in the vasopressor responses to this particular peptide (Fig. 5A, B and C), while, as for Ang I, no significant effects on HR were observed.

In addition, in WT but not mMCP-4 KO mice, C48/80 potentiated by 2.5-fold ($p=0.001$) (in terms of amplitude and duration) the pressor responses to [Pro^{11}, D-Ala^{12}] Ang I (Fig. 6A, B and C). As positive chronotropic response to the ACE-resistant analogue of Ang I was also prompted by C48/80 (Fig. 6D) in WT but not in mMCP-4 KO mice (Fig. 6C and E). Finally, cromolyn did not modify the cardiovascular responses to [Pro^{11}, D-Ala^{12}] Ang I in either mouse strains.

16

DISCUSSION

Our previous studies have demonstrated a contribution of mast cell-secreted mMCP-4 in the ECE-independent production of ET-1 in mice (Fecteau *et al.*, 2005; Simard *et al.*, 2009; Houde *et al.*, 2013). Until the present study however, it had not been established whether mast cell stability impacts on the mMCP-4-dependent biological responses to big ET-1 and Ang I *in vivo.* This study shows that induction of mast cell degranulation by C48/80 increases mMCP-4-dependent responses to exogenous big ET-1. In contrast, the mast cell stabilizer cromolyn reduced the biological activity and chymase-dependent hydrolysis of big ET-1. Further, mMCP-4 did not significantly contribute to the vasoactive properties of Ang I, suggesting an important role of mast cell stability in the ECE-independent cardiovascular properties of big ET-1 but not in the ACE-independent pressor responses to Ang I *in vivo.*

NEP is required to produce ET-1 from chymase-generated ET-1 (1-31) *in vivo* (Fecteau *et al.*, 2005). Data reported prior to this study suggested that repression of mMCP-4 in mice does not affect endothelin receptors or NEP expression in the mouse cardiovascular system (Houde *et al.*, 2013). We herein show that ET-1 (1-31) and ET-1 administration produced similar hemodynamic responses regardless of whether mast cells are activated or stabilized, illustrating that secreted mMCP-4 plays no significant role in the biological effects of these two endothelin metabolites.

The present study also argues in favor of a significant impact of mast cell stability in the production of ET-1 (1-31) *in vitro*. The loss of big ET-1 conversion

capacity in mast cells derived from mMCP-4 KO mice is correlated with the absence of chymase-like hydrolysis in the *in vitro* series of experiments using the fluorogenic substrate Suc-Leu-Leu-Val-Tyr-AMC. These results show that induction of mast cell degranulation by C48/80 leads to the release of chymase, whereas cromolyn stabilizes the mMCP-4 content within the secretory granules.

Borland *et al.* (1998) reported that, in the human saphenous vein, chymase is located within the adventitia (outer layer of the vessel) and is co-located with mast cell populations, while ACE is mainly found in the vascular endothelium. Borland *et al.* (1998) also suggested that circulating Ang I would be more accessible to ACE than to chymase. In addition, circulating chymase is rapidly and irreversibly inhibited by plasma proteins such as alpha-macroglobulins and alpha-1-antichymotrypsin, which limits the contribution of the mast cell serine protease in the production of vascular Ang II (Walter *et al.*, 1996). Tissue chymase thus is likely to be of greater importance in the functional effects of Ang II on the smooth muscle cells of blood vessel walls than in the systemic circulation (Borland *et al.*, 1998). Moreover, we previously reported no differences in the pressor responses to Ang I in non-anesthetized WT and mMCP-4 KO mice (Semaan *et al.*, 2015). In concordance with those results, we show in the present study, that modulation of mast cell degranulation does not impact the vasopressor responses to exogenous Ang I *in vivo*, suggesting that chymase may not be as biologically significant for the Ang II precursor as for big ET-1 hydrolysis in the murine systemic circulation. Given the abundance of angiotensin-converting enzyme in the mouse *in vivo* (Balcells *et al.*, 1997), it is

therefore unlikely that chymase is involved in the production of vascular Ang II under physiological or pathological conditions in mice.

In contrast, the present study suggests that chymase modulates the cardiovascular responses to the ACE-resistant analogue, [Pro^{11}, D-Ala^{12}] Ang I (Li *et al.*, 2004), in the mouse model. Using ACE inhibitors (captopril and enalapril) as well as a general inhibitor of chymotrypsin-like enzymes (chymostatin), Borland *et al.* (1998) reported a partial inhibition of the contractile properties of Ang I in human saphenous veins, suggesting the existence of both ACE- and chymase-independent pathways in the generation of Ang II. However, since several additional enzymes such as trypsin, chymotrypsin, tonin, cathepsin G and kallikrein can also generate Ang II from Ang I *in vitro* (Becari *et al.*, 2011), the contribution of these enzymes in the cardiovascular responses to Ang I remains to be investigated *in vivo*. Interestingly, the present study also reports the sensitivity of an ACE-resistant Ang I analogue ([Pro^{11}, D-Ala^{12}] Ang I) to mast cell degranulation. Specifically, [Pro^{11}, D-Ala^{12}] Ang I requires mMCP-4 for its optimal vasoactive responses and was shown to be susceptible to mast cell degranulation in the mouse model *in vivo.* Notably, the finding that cromolyn did not reduce the response to the same analogue in contrast to that of big ET-1, suggests that [Pro^{11}, D-Ala^{12}] Ang I is cleaved by interstitially located active mMCP-4 (Takai *et al.*, 2010), rather than by the same enzyme stored in mast cells.

Baroreceptors are activated by changes in blood pressure, resulting in variations in cardiac chronotropism/inotropism and systemic vascular resistance

(Guo *et al.*, 1982; Knape and van Zwieten, 1988). In this study, no effects on the heart rate were observed even at the highest doses tested of the two endogenous vasopressors big ET-1 or Ang I. In contrast, a submaximal dose (10^{-8} mol/kg) of [Pro^{11}, D-Ala^{12}] Ang I induced significant increases in HR only in C48/80 pre-treated mice, caused perhaps by higher plasma levels of chymase-produced Ang II and subsequent activation of the baroreceptor function through the Ang II type 1 receptor (AT$_1$AR) (Wong *et al.*, 1993; Matsumura *et al.*, 1999).

A significant role for mMCP-4 in a mouse model of experimental autoimmune encephalomyelitis (EAE), was recently reported by our laboratory (Desbiens *et al.*, 2016, 2019). Those studies showed an increase in the mMCP-4-dependent production of ET-1 in the periphery and the central nervous system. More recently, Pinke *et al.* (2020) showed that mast cell stabilization with ketotifen lowered disease prevalence and severity and the expression of chymase and carboxypeptidase A in mice, thus supporting a potentially therapeutic indication for mast cell stabilizers in multiple sclerosis (Pinke *et al.*, 2020). Deleterious roles for mast cell-derived chymase have also been shown in experimental models of cardiac infarct, ischemia/reperfusion, and atherosclerosis (Jin, 2003; Tejada *et al.*, 2016; Houde *et al.*, 2018). Finally, patients with myocardial infarction show increased levels of plasmatic and cardiac ET-1 (1-31) and chymase activity in the same organ (Oka *et al.*, 2014). Whether increased chymase production prompted by mast cells activation under inflammatory conditions is correlated with enhanced production of ET-1 levels in cardiovascular diseases however, remains to be investigated.

Vascular or autoimmune diseases in which inflammatory processes associated with mast cell activation have been documented (Hermans *et al.*, 2019; Kempuraj *et al.*, 2020) and interestingly, also recently reported in post-COVID-19 patients (Afrin *et al.*, 2020). Furthermore, Ahmad *et al.* (2019) suggested that stabilizing mast cells could prevent cardiac remodeling since chymase has a high affinity for the human Ang I peptide, *in vitro*. Agents enhancing mast cell stability may thus have beneficiary effects by reducing the deleterious contribution of chymase, Ang II and as shown in this study, ET-1, in pro-inflammatory cardiac and vascular disorders.

ACKNOWLEDGEMENTS

AUTHORSHIP CONTRIBUTIONS

Participated in research design: Vincent, Lapointe, D'Orléans-Juste

Conducted experiments: Vincent, Lo, Gagnon

Performed data analysis: Vincent, Gagnon

Contributed new reagents or analytic tools: Pejler, Takai, Day, D'Orléans-Juste

Wrote or contributed to the writing of the manuscript: Vincent, Lapointe, Pejler,

D'Orléans-Juste

CONFLICT OF INTERESTS

The authors declare that there is no conflict of interest regarding the publication

of this manuscript.

REFERENCES

Ahmad S, Wright KN, Sun X, Groban L, and Ferrario CM (2019) Mast cell peptidases (carboxypeptidase A and chymase)-mediated hydrolysis of human angiotensin-(1–12) substrate. *Biochem Biophys Res Commun* **518**: 651–656.

Akasu M, Urata H, Kinoshita A, Sasaguri M, Ideishi M, and Arakawa K (1998) Differences in Tissue Angiotensin II–Forming Pathways by Species and Organs In Vitro. *Hypertension* **32**: 514–520.

Afrin LB, Weinstock LB, and Molderings GJ (2020) Covid-19 hyperinflammation and post-Covid-19 illness may be rooted in mast cell activation syndrome. *Int J Infect Dis* **100**: 327–332.

Balcells E, Meng QC, Johnson WH, Oparil S, and Dell'Italia LJ (1997) Angiotensin II formation from ACE and chymase in human and animal hearts: methods and species considerations. *Am J Physiol-Heart C* **273**: H1769–H1774.

Becari C, Oliveira EB, and Salgado MCO (2011) Alternative pathways for angiotensin II generation in the cardiovascular system. *Braz J Med Biol Res* **44**: 914–919.

Blank U (2011) The mechanisms of exocytosis in mast cells. *Adv Exp Med Biol* **716**: 107–122.

Borland JA, Chester AH, Morrison KA, and Yacoub MH (1998) Alternative pathways of angiotensin II production in the human saphenous vein. *Br J Pharmacol* **125**: 423–428.

Company C, Piqueras L, Naim Abu Nabah Y, Escudero P, Blanes JI, Jose PJ, Morcillo EJ, and Sanz M-J (2011) Contributions of ACE and mast cell chymase to endogenous angiotensin II generation and leucocyte recruitment in vivo. *Cardiovasc Res* **92**: 48–56.

Davenport AP, Hyndman KA, Dhaun N, Southan C, Kohan DE, Pollock JS, Pollock DM, Webb DJ, and Maguire JJ (2016) Endothelin. *Pharmacol Rev* **68**: 357–418.

Desbiens L, Lapointe C, Gharagozloo M, Mahmoud S, Pejler G, Gris D, and D'Orléans-Juste P (2016) Significant Contribution of Mouse Mast Cell Protease 4 in Early Phases of Experimental Autoimmune Encephalomyelitis. *Mediators Inflamm* **2016**: 1–10.

Desbiens L, Lapointe C, Gendron L, Gharagozloo M, Vincent L, Pejler G, Gris D, and D'Orléans-Juste P (2019) Experimental Autoimmune Encephalomyelitis Potentiates Mouse Mast Cell Protease 4–Dependent Pressor Responses to Centrally or Systemically Administered Big Endothelin-1. *J Pharmacol Exp Ther* **370**: 437–446.

D'Orléans-Juste P, Houde M, Rae GA, Bkaily G, Carrier E, and Simard E (2008) Endothelin-1 (1-31): from chymase-dependent synthesis to cardiovascular pathologies. *Vascul Pharmacol* **49**: 51–62.

Fecteau M-H, Honoré J-C, Plante M, Labonté J, Rae GA, and D'Orléans-Juste P (2005) Endothelin-1 (1-31) is an intermediate in the production of endothelin-1 after big endothelin-1 administration in vivo. *Hypertension* **46**: 87–92.

Fleming I (2006) Signaling by the Angiotensin-Converting Enzyme. *Circ Res* **98**: 887–896.

Hermans M, Lennep JR van, van Daele P, and Bot I (2019) Mast Cells in Cardiovascular Disease: From Bench to Bedside. *Int J Mol Sci* **20**: 3395.

Houde M, Jamain M-D, Labonté J, Desbiens L, Pejler G, Gurish M, Takai S, and D'Orléans-Juste P (2013) Pivotal role of mouse mast cell protease 4 in the conversion and pressor properties of Big-endothelin-1. *J Pharmacol Exp Ther* **346**: 31–37.

Houde M, Schwertani A, Touil H, Desbiens L, Sarrhini O, Lecomte R, Lepage M, Gagnon H, Takai S, Pejler G, *et al.* (2018) Mouse Mast Cell Protease 4 Deletion Protects Heart Function and Survival After Permanent Myocardial Infarction. *Front Pharmacol* **9**: 868.

Irman-Florjanc T and Erjavec F (1983) Compound 48/80 and substance P induced release of histamine and serotonin from rat peritoneal mast cells. *Agents Actions* **13**: 138–141.

Jin D (2003) Impact of chymase inhibitor on cardiac function and survival after myocardial infarction. *Cardiovasc Res* **60**: 413–420.

Kempuraj D, Ahmed ME, Selvakumar GP, Thangavel R, Raikwar SP, Zaheer SA, Iyer SS, Govindarajan R, Nattanmai Chandrasekaran P, Burton C, *et al.* (2020) Acute Traumatic Brain Injury-Induced Neuroinflammatory Response and Neurovascular Disorders in the Brain. *Neurotox Res* 1-10.

Knape JTA, and van Zwieten PA (1988) Positive chronotropic activity of angiotensin II in the pithed normotensive rat is primarily due to activation of cardiac β1-adrenoceptors. *Naunyn-Schmiedeberg's Arch Pharmacol* **338**: 185–190.

Koide Y, Tatsui A, Hasegawa T, Murakami A, Satoh S, Yamada H, Kazayama S, and Takahashi A (2003) Identification of a stable chymase inhibitor using a pharmacophore-Based database search. *Bioorg Med Chem Lett* **13**: 25–29.

Kunori Y, Muroga Y, Iidaka M, Mitsuhashi H, Kamimura T, and Fukamizu A (2005) Species Differences in Angiotensin II Generation and Degradation by Mast Cell Chymases. *J Recept Sig Transd* **25**: 35–44.

Li M, Liu K, Michalicek J, Angus JA, Hunt JE, Dell'Italia LJ, Feneley MP, Graham RM, and Husain A (2004) Involvement of chymase-mediated angiotensin II generation in blood pressure regulation. *J Clin Invest* **114**: 112–120.

McDonald JE, Padmanabhan N, Petrie MC, Hillier C, Connell JM, and McMurray JJ (2001) Vasoconstrictor effect of the angiotensin-converting enzyme-

resistant, chymase-specific substrate [Pro(11)(D)-Ala(12)] angiotensin I in human dorsal hand veins: in vivo demonstration of non-ace production of angiotensin II in humans. *Circulation* **104**: 1805–1808.

McMahon EG, Palomo MA, Moore WM, McDonald JF, and Stern MK (1991) Phosphoramidon blocks the pressor activity of porcine big endothelin-1-(1-39) in vivo and conversion of big endothelin-1-(1-39) to endothelin-1-(1-21) in vitro. *Proc Natl Acad Sci USA* **88**: 703–707.

Moore JE and James GW (1953) A simple direct method for absolute basophil leucocyte count. *Proc Soc Exp Biol Med* **82**: 601–603.

Nakano A, Kishi F, Minami K, Wakabayashi H, Nakaya Y, and Kido H (1997) Selective conversion of big endothelins to tracheal smooth muscle-constricting 31-amino acid-length endothelins by chymase from human mast cells. *J Immunol* **159**: 1987–1992.

Oka M, Niwa Y, Mawatari K, Hiasa Y, and Nakaya Y (2014) A novel peptide of endothelin family, 31 amino-acid length endothelin in patients with acute myocardial infarction. *J Med Invest* **61**: 298–305.

Pejler G, Ronnberg E, Waern I, and Wernersson S (2010) Mast cell proteases: multifaceted regulators of inflammatory disease. *Blood* **115**: 4981–4990.

Pinke KH, Zorzella-Pezavento SFG, de Campos Fraga-Silva TF, Mimura LAN, de Oliveira LRC, Ishikawa LLW, Fernandes AAH, Lara VS, and Sartori A

(2020) Calming Down Mast Cells with Ketotifen: A Potential Strategy for Multiple Sclerosis Therapy? *Neurotherapeutics* **17**: 218–234.

Röhlich P, Anderson P, and Uvnäs B (1971) Electron microscope observations on compounds 48-80-induced degranulation in rat mast cells. Evidence for sequential exocytosis of storage granules. *J Cell Biol* **51**: 465–483.

Rossi G (1999) Interactions between endothelin-1 and the renin–angiotensin–aldosterone system. *Cardiovasc Res* **43**: 300–307.

Samoszuk M and Corwin MA (2003) Mast cell inhibitor cromolyn increases blood clotting and hypoxia in murine breast cancer. *Int J Cancer* **107**: 159–163.

Semaan W, Desbiens L, Houde M, Labonté J, Gagnon H, Yamamoto D, Takai S, Laidlaw T, Bkaily G, Schwertani A, *et al.* (2015) Chymase inhibitor-sensitive synthesis of endothelin-1 (1-31) by recombinant mouse mast cell protease 4 and human chymase. *Biochem Pharmacol* **94**: 91–100.

Simard E, Jin D, Takai S, Miyazaki M, Brochu I, and D'Orléans-Juste P (2009) Chymase-dependent conversion of Big endothelin-1 in the mouse in vivo. *J Pharmacol Exp Ther* **328**: 540–548.

Skedinger MC, Augustine NH, Morris EZ, Nielson DW, Zimmerman GA, and Hill HR (1987) Effect of disodium cromoglycate on neutrophil movement and intracellular calcium mobilization. *J Allergy Clin Immunol* **80**: 573–577.

Takai S, Jin D, and Miyazaki M (2010) New approaches to blockade of the renin-angiotensin-aldosterone system: chymase as an important target to prevent organ damage. *J Pharmacol Sci* **113**: 301–309.

Tariq M, Moutaery MA, Elfaki I, Arshaduddin M, and Khan HA (2006) Protective effects of nedocromil sodium and sodium cromoglycate on gastroduodenal ulcers: a comparative study in rats. *Inflammopharmacology* **14**: 163–169.

Tchougounova E, Pejler G, and Åbrink M (2003) The Chymase, Mouse Mast Cell Protease 4, Constitutes the Major Chymotrypsin-like Activity in Peritoneum and Ear Tissue. A Role for Mouse Mast Cell Protease 4 in Thrombin Regulation and Fibronectin Turnover. *J Exp Med* **198**: 423–431.

Tejada T, Tan L, Torres RA, Calvert JW, Lambert JP, Zaidi M, Husain M, Berce MD, Naib H, Pejler G, *et al.* (2016) IGF-1 degradation by mouse mast cell protease 4 promotes cell death and adverse cardiac remodeling days after a myocardial infarction. *Proc Natl Acad Sci USA* **113**: 6949–6954.

Walter M, Plotnick M, and Schechter NM (1996) Inhibition of human mast cell chymase by secretory leukocyte proteinase inhibitor: enhancement of the interaction by heparin. *Arch Biochem Biophys* **327**: 81–88.

Xu D, Emoto N, Giaid A, Slaughter C, Kaw S, deWit D, and Yanagisawa M (1994) ECE-1: a membrane-bound metalloprotease that catalyzes the proteolytic activation of big endothelin-1. *Cell* **78**: 473–485.

Wong J, Chou L, and Reid IA (1993) Role of AT1 receptors in the resetting of the
baroreflex control of heart rate by angiotensin II in the rabbit. *J Clin Invest* **91**:
1516–1520.

FOOTNOTES

FIGURE LEGENDS

Figure 1. Maximal variation in mean arterial pressure (ΔMAP) following IV administration of big ET-1 in WT (A) and mMCP-4 KO (B) mice pre-treated with either vehicle, C48/80 or cromolyn; Time course of the ΔMAP in response to IV administration of a single dose of big ET-1 (1 nmol/kg) in WT (C) and mMCP-4 KO (D) mice pre-treated with the above-mentioned agents, and their respective heart rate (HR) (E-F). Each point corresponds to the mean ± S.E.M. of the MAP increase. (n=6-10). *p<0.05; **p<0.01; ***p<0.001 vs. WT + vehicle by one-way ANOVA with Dunnett's multiple comparison test.

Figure 2. (A) Maximal variation in mean arterial pressure (ΔMAP) in response to big ET-1 (1 nmol/kg) in WT mice pre-treated IV with vehicle or TY-51469 (10 mg/kg); (B) Maximal ΔMAP following IV administration of ET-1 (1-31) (1 nmol/kg) and ET-1 (0.5 nmol/kg) in WT mice. Each bar corresponds to the mean ± S.E.M. of the MAP increase *(n=5-9). *p<0.05; ***p<0.001 vs. WT + vehicle by one-way ANOVA with Dunnett's multiple comparison test.

Figure 3. (A) Quantification of the specific cleavage of the fluorogenic substrate Suc-Leu-Leu-Val-Tyr-AMC by recombinant mMCP-4 (rmMCP-4, 154.32 nM) in the presence of vehicle, C48/80 (12 µM), cromolyn (600 µM), or TY-51469 (10 µM) (n=6); (B) Quantification of the specific AMC cleavage of the fluorogenic substrate measured *ex vivo* in mast cells derived from WT (pre-treated with vehicle, C48/80 or cromolyn) or mMCP-4 KO peritoneal mast cells extracts (n=6-10); (C) *In vitro* conversion of big ET-1 into ET-1 (1–31) from intact peritoneal

mast cells derived from WT or mMCP-4 KO in presence of vehicle, C48/80 (1 µM) or cromolyn (20 µM) using Mass Spectrometry area under the curve arbitrary units (AU) (n=4-5). Each point and bar correspond to the mean ± S.E.M. *p<0.05; ***p<0.001 vs. rmMCP-4 or WT + vehicle by one-way ANOVA with Dunnett's multiple comparison test.

Figure 4. (A) Maximal variation in mean arterial pressure (ΔMAP) following the IV administration of Ang I in WT and mMCP-4 KO mice; Time course of the variation of the Δ MAP in response to IV administration of Ang I (0.01 nmol/kg) in WT (B) and mMCP-4 KO mice (C) pre-treated with vehicle, C48/80 or cromolyn, and their respective heart rate (HR) (C-D). Each point and bar correspond to the mean ± S.E.M. of the MAP increase of 6-8 separate experiments.

Figure 5. (A) Dose-response curves (area under the curve (AUC)) of the Angiotensin-converting enzyme (ACE)-resistant analogue ([Pro[11], D-Ala[12]] Ang I) in WT and mMCP-4 KO mice (n=4-9); Time course of maximal variation in mean arterial pressure (ΔMAP) in response to IV administration of [Pro[11], D-Ala[12]] Ang I [(B) 10 nmol/kg (n=8-9); (C) 20 nmol/kg (n=9)] in WT and mMCP-4 KO mice, and their respective heart rate (HR) (D-E). Each point corresponds to the mean ± S.E.M. of the MAP increase. *p<0.05; ***p<0.001 vs. WT + vehicle by Student's t test.

Figure 6. (A) Time course (area under the curve (AUC)) of [Pro[11], D-Ala[12]] Ang I (10 nmol/kg) in WT or mMCP-4 KO mice pre-treated with either vehicle, C48/80 or cromolyn; Maximal variation in mean arterial pressure (ΔMAP) in response to

IV administration of [Pro^{11}, D-Ala^{12}] Ang I in (B) WT and (C) mMCP-4 KO mice, and their respective heart rate (HR) (D-E). Each point and bar correspond to the mean ± S.E.M. of 7-8 separate experiments. *$p<0.05$; **$p<0.01$ vs. WT + vehicle by one-way ANOVA with Dunnett's multiple comparison test (A) and Student's t test (B, D).

Figure 1

Figure 2

Figure 3

A

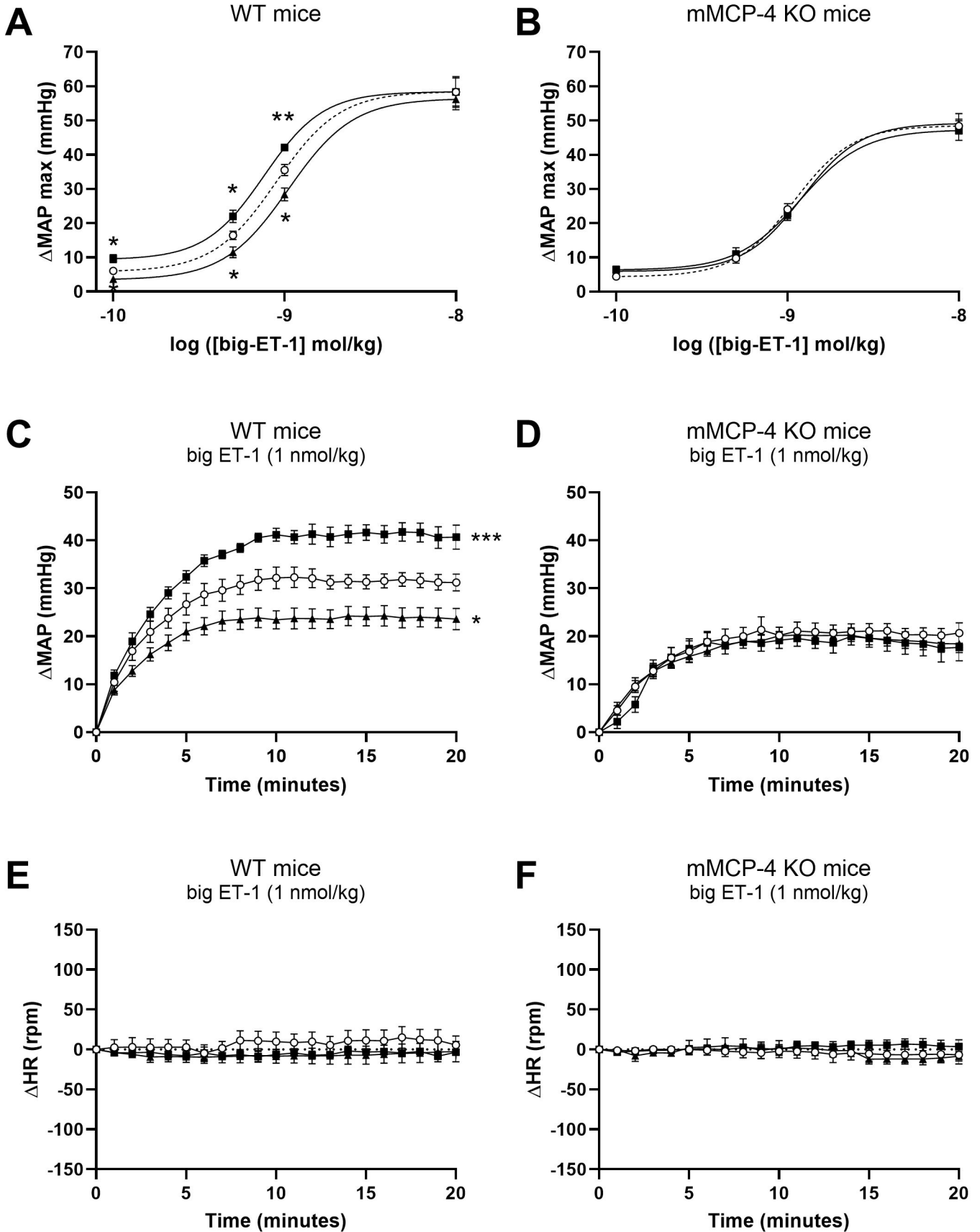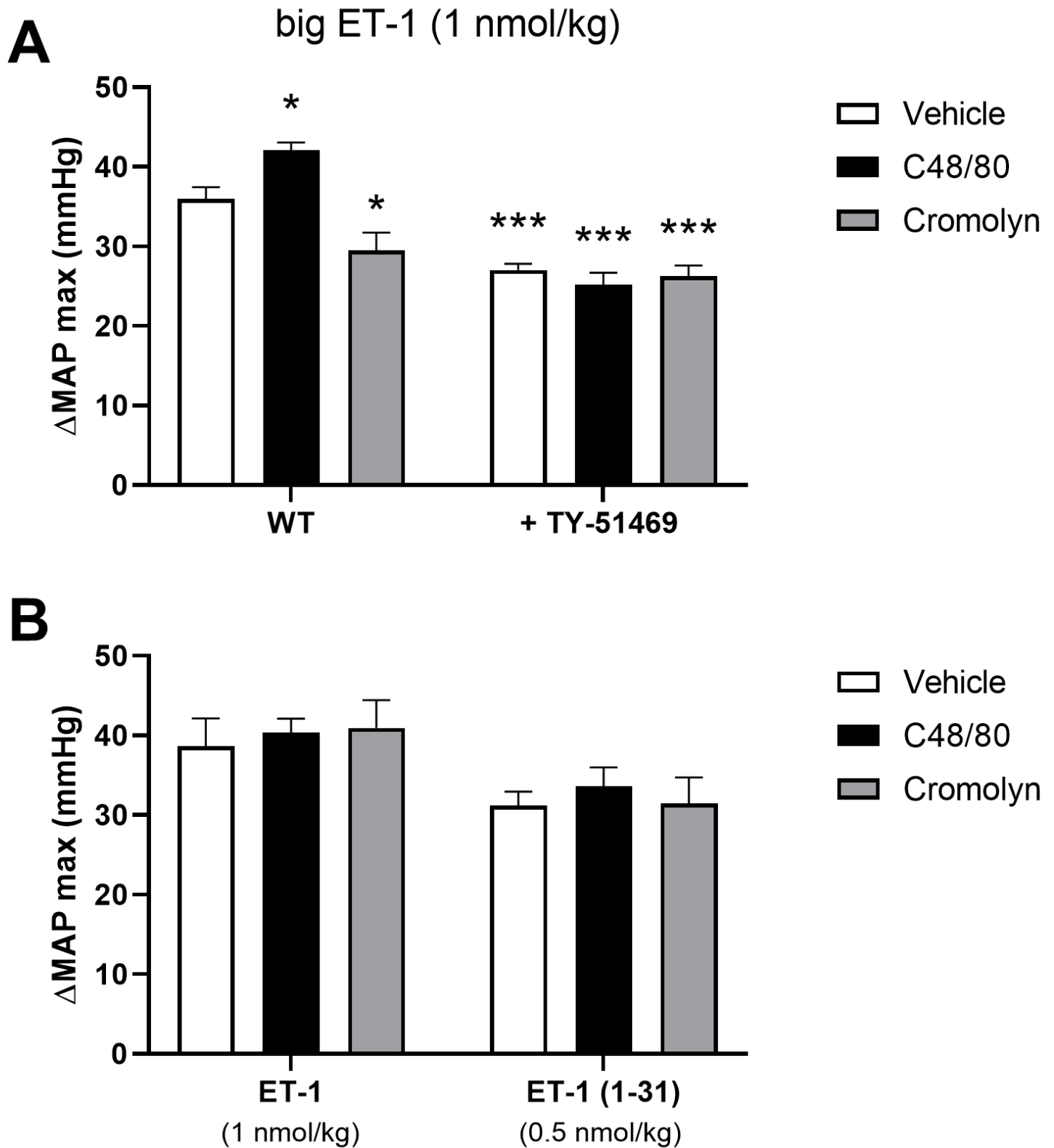**Recombinant mMCP-4 (154.32 nM)**

Bar chart. Y-axis: Maximal AMC specific cleavage (nM), scale 0–12. X-axis categories: Vehicle, + C48/80, + Cromolyn, + TY-51469. The + TY-51469 bar is marked ***.

B

Mast cells (10^5 cells)

Line graph. Y-axis: AMC specific cleavage (nM), scale 0–12. X-axis: Time (minutes), 0–20. Legend: WT (open circle), + C48/80 (filled square), + Cromolyn (filled triangle), mMCP-4 KO (circle with dot). Markings: * near Cromolyn, *** near + C48/80, *** near mMCP-4 KO.

C

Bar chart. Y-axis: ET-1 (1-31) (Peak area), scale 0–150000. X-axis categories: Vehicle, C48/80, Cromolyn (under WT mast cells); Vehicle, C48/80 (under mMCP-4 KO mast cells). Markings: C48/80 (WT) ***, Cromolyn (WT) *, Vehicle (KO) ***, C48/80 (KO) ***.
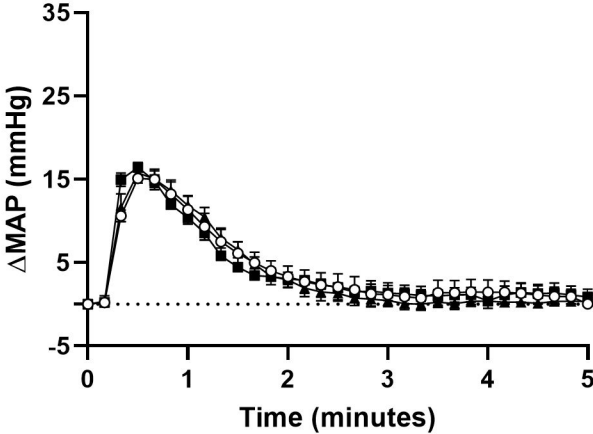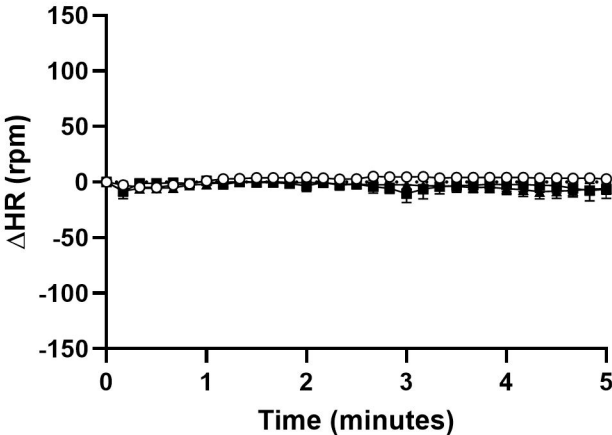
Figure 4

A Ang I

B WT mice
Ang I (0.01 nmol/kg)

C mMCP-4 KO mice
Ang I (0.01 nmol/kg)

D WT mice
Ang I (0.01 nmol/kg)
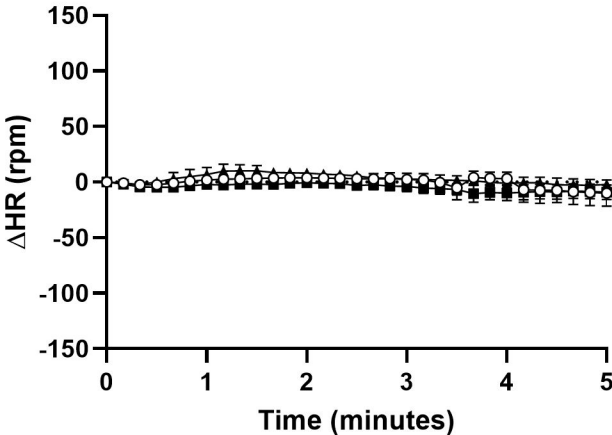
E mMCP-4 KO mice
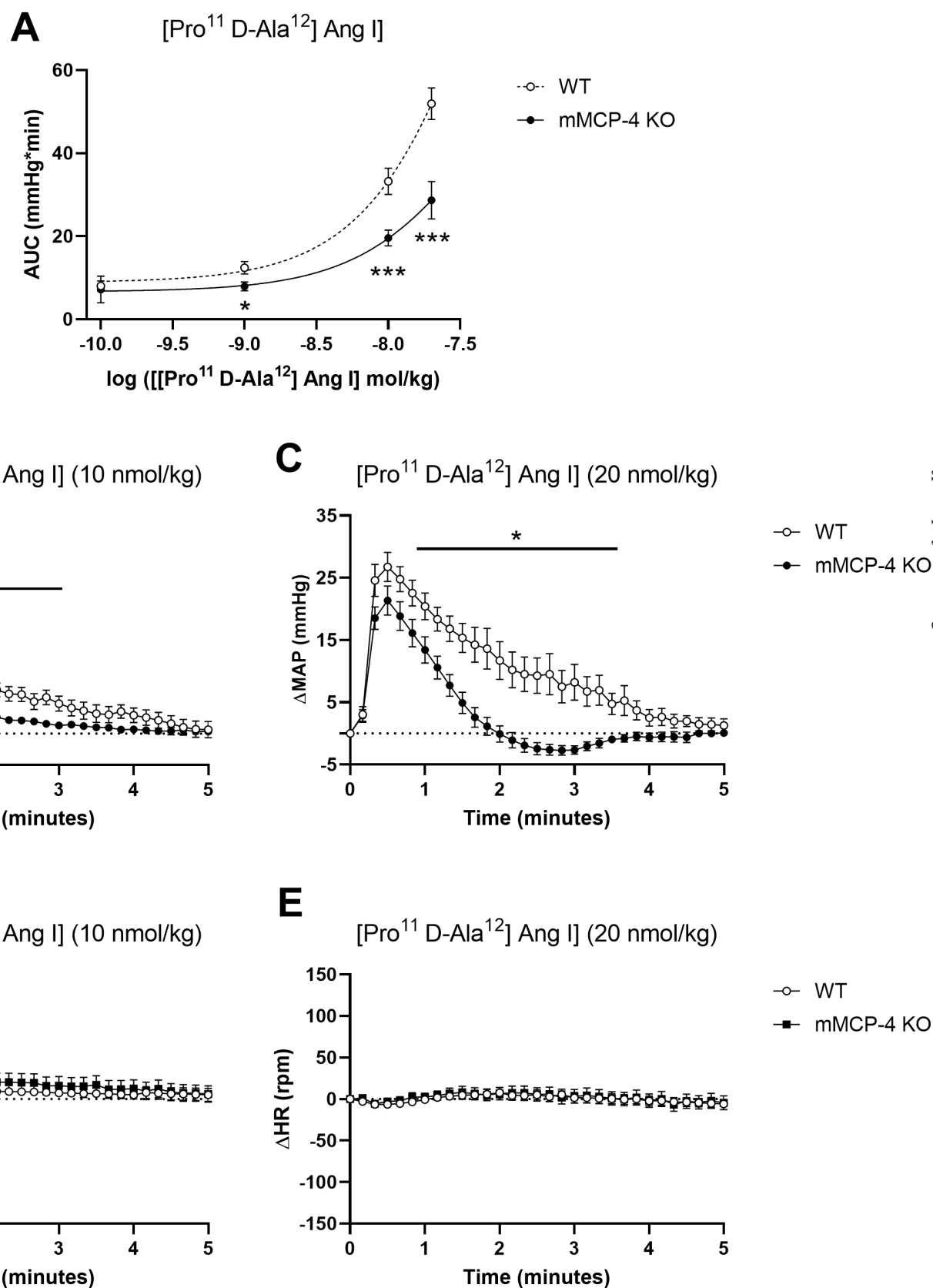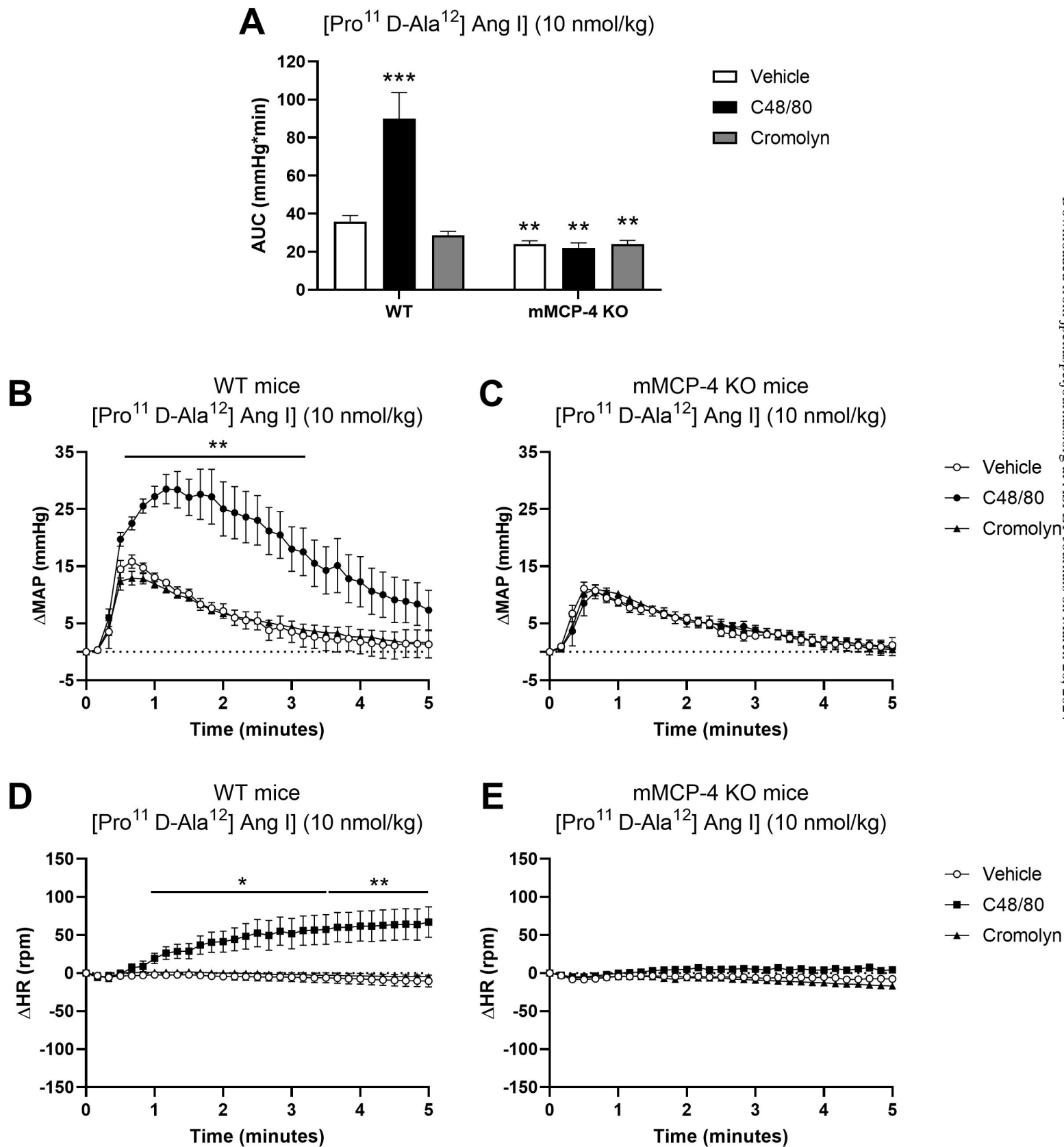Ang I (0.01 nmol/kg)

Figure 5

Figure 6

SUPPLEMENTARY DATA

JPET-AR-2020-000325
Mast cell degranulation increases mouse Mast Cell Protease 4-dependent
vasopressor responses to big endothelin-1 but not Angiotensin I. (Vincent et al)

Table S1. Basal hemodynamic parameters in anesthetized mice treated with C480/80 or cromolyn.

Hemodynamic parameters	WT mice			mMCP-4 KO mice		
	Vehicle	C48/80	Cromolyn	Vehicle	C48/80	Cromolyn
MAP (mmHg)	57.8 ± 2.8	64.2 ± 3.3	63.4 ± 3.7	62.0 ± 3.9	64.5 ± 2.1	60.1 ± 1.9
Systolic (mmHg)	70.7 ± 3.0	76.8 ± 2.2	74.8 ± 4.0	72.7 ± 4.0	73.4 ± 2.2	72.1 ± 2.5
Diastolic (mmHg)	47.8 ± 2.8	49.8 ± 3.2	51.6 ± 3.5	50.5 ± 3.9	53.1 ± 3.0	48.5 ± 1.7
Heart Rate (bpm)	221.6 ± 15.7	214.4 ± 18.7	232.5 ± 23.7	215.2 ± 25.0	208.9 ± 15.0	196.4 ± 13.1
Pulse pressure (mmHg)	25.0 ± 2.1	28.7 ± 2.2	24.3 ± 2.1	22.2 ± 2.0	22.0 ± 2.33	23.6 ± 1.3

All mice were anesthetized with ketamine/xylazine (87/13 mg/kg). Data are expressed as mean ± SEM of at least 6 separate experiments.
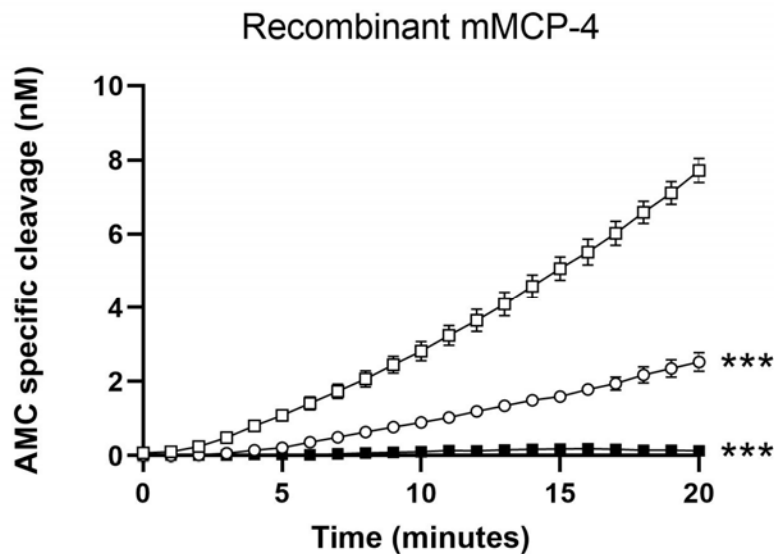
Figure S1. Quantification of the specific cleavage of the fluorogenic substrate Suc-Leu-Leu-Val-Tyr-AMC by the recombinant mMCP-4 (rmMCP-4, 30.86 nM (○) or 154.32 nM (□)) + vehicle or rmMCP-4 (154.32 nM) + TY-51469 (10 μM) (■). Each point represents the average $\pm$ SEM of 6 different experiments. ***$p<0.001$ vs. rmMCP-4 (154.32 nM) + vehicle by one-way ANOVA with Dunnett's multiple comparison test.